Ocean Engineering 142 (2017) 292–302

Contents lists available at ScienceDirect

Ocean Engineering

journal homepage: www.elsevier.com/locate/oceaneng

Study of manipulator operations maneuvered by a ROV in virtual environments☆

Jin Zhang[a,b], Wei Li[a,c,*], Jiancheng Yu[a], Xisheng Feng[a], Qifeng Zhang[a], Genshe Chen[d]

[a] Robotics State Key Laboratory, Shenyang Institute of Automation, Chinese Academy of Sciences, Shenyang 110016, China
[b] University of Chinese Academy of Sciences, Beijing 100049, China
[c] Department of Computer & Electrical Engineering and Computer Science, California State University, Bakersfield, CA 93311, USA
[d] Intelligent Fusion Technology, Inc, Germantown, MD 20876, USA

ARTICLE INFO

Keywords:
Autonomous operation
Remote operation
Underwater manipulator operations
Virtual ROV

ABSTRACT

It is extremely difficult to operate an underwater manipulator carried on a remotely operated vehicle (ROV) in the deep sea. In order to investigate underwater manipulator operations maneuvered by a remotely operated vehicle (ROV), this paper develops a virtual underwater manipulator and its carrier, the ROV, via the three-dimensional simulator "Webots" to animate operational tasks. The ROV model refers to the structure of a typical ROV which operates below the ocean's surface down to 1000 m, while the graphical and kinematic models of the manipulator refer to a master-slave servo hydraulic manipulator with 7 functions, consisting of six degrees of freedom (DOFs) and a parallel gripper for manipulations. This study uses the virtual platform to challenge an operator to conduct different tasks by using the manipulator, including two switch-based and one master arm-based operation, and combined by remote and autonomous operations. When conducting the operations, we have considered uncertain external disturbances that stem from subsea environments. In order to demonstrate the feasibility and effectiveness of the virtual platform, we have designed two typical underwater operational tasks for training the operator: grasping a machine part in a basket, and making a circle at a specified position on the seabed. The tasks are completed by coordinating the underwater manipulator, the submersible vehicle, and a pan-tilt camera. Three operators were invited for the training operations, and their operating results are presented.

1. Introduction

A ROV, which plays an important role in underwater operations, mainly consists of a submersible vehicle, an umbilical cable, and a surface console. Because the ROV is able to run in deep and dangerous underwater environments for a long time to conduct operations with high intensity and large quantity, it has been widely used for observing ocean environments, exploiting marine resources, inspecting and maintaining underwater platforms, etc. (Lorance and Trenkel, 2006; Park et al., 2011; Narayanaswamy et al., 2013; Wang et al., 2016). An operator performs diverse underwater operational tasks based on live videos of the surrounding environment sent back to the surface console (located on the ground or on a ship). The important part in such an operating system includes the manipulator and operational tools carried by the ROV (Yan et al., 2005).

Operating the manipulator carried by the ROV to perform operational tasks in the deep sea is very challenging, because the underwater environment is complex and uncertain. A qualified operator needs to go through a comprehensive training process before operating the underwater manipulator carried by the ROV. The existing real ROV systems usually present only their functions and service purposes (SeaVeyors Environmental and Marine Services Limited, 2015; Zhang et al., 2014), but they rarely deliver their operating processes in detail and report operation results' analysis, and in particular they do not specify how to coordinately operate each component of the ROV systems when conducting the operational tasks, so these real ROV systems cannot be served as references for training operators. It is also not convenient to adjust external disturbances and operational modes to their manipulators to train operators. In addition, training the operator by using a real ROV is time-consuming, expensive and dangerous. Therefore, the study addressed in this paper is to establish a training platform, consisting of a virtual underwater manipulator and its carrier

☆ This work was supported in part by The Key Research Project of Frontier Science, Chinese Academy of Sciences (Grant No. QYZDY-SSW-JSC005), by The National Key Research and Development Program of China (Grant No. 2016YFC0300801), and by The National Natural Science Foundation of China (Grant No. 61473207 and 61233013).

* Corresponding author at: Department of Computer & Electrical Engineering and Computer Science, California State University, Bakersfield, CA 93311, USA.
E-mail addresses: zhangjin1@sia.cn (J. Zhang), wli@csub.edu (W. Li), yjc@sia.cn (J. Yu), fxs@sia.cn (X. Feng), zqf@sia.cn (Q. Zhang), gchen@intfusiontech.com (G. Chen).

http://dx.doi.org/10.1016/j.oceaneng.2017.07.008
Received 30 March 2017; Received in revised form 27 May 2017; Accepted 2 July 2017

– ROV, for the operator to realistically simulate the processes of underwater operations in the deep sea environment. This effective training platform teaches the operator the operational requirements, lets them become familiar with operational processes, helps to improve operational skills, reduces the cost and risk in the experiment, and enhances safety awareness. GRI Simulations Inc. developed a ROV virtual platform in VROV simulator, carrying a virtual manipulator based on the structure of TITAN 4, using a master arm as a training tool for an operator (GRI Simulations Inc, 2015). GRI as a commercial company is costly when using its virtual platform. Especially, when you consider that this system does not provide the training process and setting procedure for operational tasks. In addition, it only provides a single operational mode: master arm-based manipulator operation, so it is not suitable for investigating and comparing a variety of underwater manipulator operational modes. The work in Hamzah et al. (2008) constructed a virtual ROV used for inspecting pipelines, but the structure of the virtual ROV seems too simple to incorporate with a manipulator to carry out complex and diverse underwater operations. The virtual ROV constructed in Chi (2013) was used for training an operator to perform some operational tasks, however, its underwater manipulator did not mount on a ROV when carrying out underwater operations. To the best of our knowledge, there are no published works that have documented a virtual ROV with a mounted underwater manipulator used for comprehensively training an operator. Specifically, there are no platforms providing the operating process and setting procedure of training an operator using a virtual or real underwater manipulator designed for a ROV and comparing the operational performance.

In this paper, we used the 3D robot simulation software package – Webots (Michel, 2004; Webots) to develop the virtual platform of the underwater manipulator and its carrier – ROV provides an operator with a low-cost, safe, and conveniently configurable training platform. The virtual platform delivered four operational modes for training: remotely operate the manipulator joints through the keyboard, remotely operate the pose position and orientation of the end-effector through the keyboard, remotely operate the manipulator through the master arm, and operate the manipulator by combining remote operation with autonomous operation through the keyboard. In order to demonstrate the feasibility and effectiveness of the virtual platform, we have designed two typical underwater operational tasks for training different operational modes of the manipulator: grasping a machine part in a basket, and making a circle at a specified position on the seabed. An operator can practice how to coordinate the underwater manipulator, the submersible vehicle and the pan-tilt camera for accomplishing operational tasks. Three operators were invited for the training operations, and their operating process and results were presented. We considered some external disturbances while training the operator. This platform is able to serve as a preliminary validation tool to test the motion control methods of ROVs and manipulators in the real world (Jun et al., 2008; Koivumäki and Mattila, 2016; Shim et al., 2010).

2. Development of the virtual platform

Webots is a professional mobile robot simulation software package, developed by Cyberbotics Ltd, for fast prototyping and realistically simulating mobile robots. It allows a user to create 3D virtual worlds with physical properties and equip these robots with a number of sensors and actuator devices. In this paper, we use Webots to develop the virtual platform.

The ROV refers to the structure of a typical ROV which can operate below the ocean's surface to a depth of 1000 m. Its movement can be controlled with six degrees of freedom in three dimensional space, which includes three translational motions (surge, heave and sway) and three rotational motions (roll, pitch and yaw). Fig. 1 shows the views of the ROV from lateral, front, top, and bottom. The virtual ROV is composed of the seven main components: buoyancy modules, bearing frame, propulsion modules, sealed cabin, umbilical cable, auxiliary fittings, and an underwater manipulator with seven functions. The buoyancy modules, including frontside and backside buoyancy materials, are located on the top of the ROV to produce sufficient buoyancy. The bearing frame is the main load-bearing body for launching and retrieving the ROV and the base for mounting ROV system equipment, such as the buoyancy blocks, the sealed cabin, operation tools, etc. The propulsion module is composed of seven propellers to ensure the agility of the ROV in 3D, including four horizontal direction propellers and three vertical direction propellers. The underwater manipulator with seven functions is located in the lower-front of the ROV at its initial pose, and is an indispensable tool for underwater operations. The sealed cabin is located at the upper-back of the ROV, and is used to protect the internal electronic components and detection equipment. The umbilical cable is located on the top of the ROV and connected to the bearing frame, and is used to provide power for the submersible vehicle and to establish communications between the submersible vehicle and the console. The auxiliary fittings distributed over the bearing frame mainly include motor pumps, valve boxes, junction boxes, branch boxes, compensators, headlamps, pan-tilt and camera, sensors, etc.

A scene tree graphically represents a simulated world, including robots and the environment. A list of nodes is organized in hierarchical structures. Each node contains fields, and the fields contain other nodes. We implemented the ROV virtual model by adding and expanding a Robot node and populating its child node list with all the components of the ROV.

The geometry and appearance of each component are defined by its Shape node. We add a Geometry node as the geometry field of each created Shape node. The sealed cabin, umbilical cable and some parts of the auxiliary accessories are constructed by geometric primitive nodes: Box node, Capsule node, Cylinder node, etc., due to their simple structures. In contrast, for the components with complex structures, such as the buoyancy material, underwater manipulator, propellers, etc., irregular polyhedrons are needed to compose them. It's a complicated process to construct the complex structures, we used the following two ways to construct them: (1) Using the IndexedFaceSet node, which represents a 3D shape formed by polygons with a list of vertices; (2) Using a third-party software, SolidWorks, to model them as VRML97 format and to import them into the Webots environments. We added an Appearance node as the appearance field of each created Shape node, and then added a Material node to the material field of each created Appearance node. The visual attributes (color, brightness, texture, etc.) of all the components are specified by their Material nodes. We made the color of the buoyancy material yellow by setting its Material node as follows: ambient Intensity field to 1; diffuse Color field to (0.28, 0.28, 0.0); emissive Color field to (0.04, 0.04, 0.04); shininess field to 0.4; specular Color field to (0.5 0.5, 0); transparency field to 0; texture field to NULL. We modified the visual attributes of other components similarly. The position and orientation of each component can be modified by the translation and rotation fields in Solid nodes. A Transform node, including a translation vector and a rotation matrix, is usually used to configure the relative position and orientation of each component. Other attributes, such as physical properties, whether physical boundaries can be moved or not, and whether they can also be applied to each component by modifying corresponding fields in Solid nodes.

A Servo node added to a joint forms a DOF for a mechanical simulation. The joint placed between the parent and child nodes move the child objects with respect to their direct parent. The type field is a string which specifies the Servo type, and may be either “rotational” (default) or “linear”. A “rotational” Servo is used to simulate a rotating motion, and a “linear” Servo is used to simulate a sliding motion. We applied a “rotational” Servo to each propeller to simulate its rotation, three “rotational” Servos and three “linear” Servos to simulate ROV's

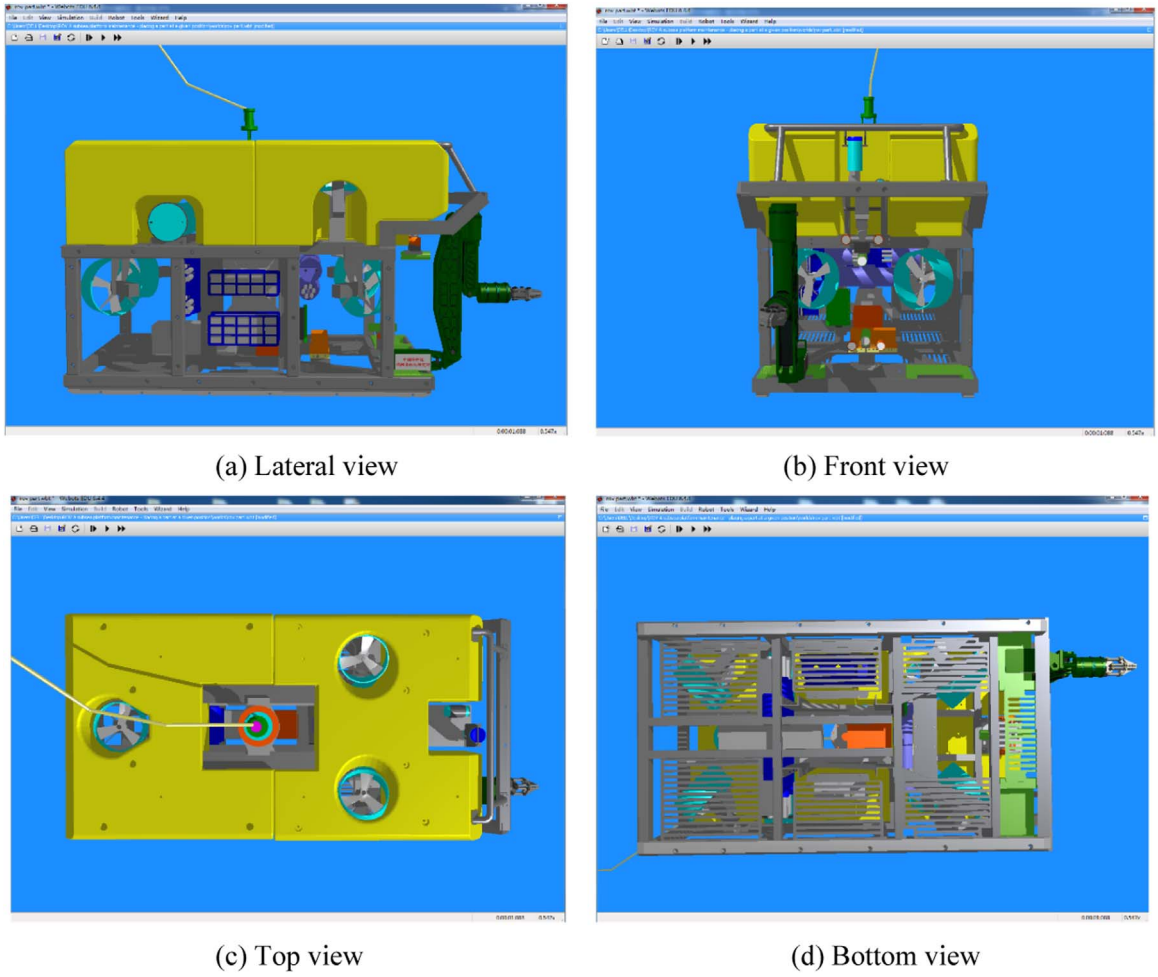

Fig. 1. The virtual ROV.

rotations and translations along the x, y, and z axes, two “rotational” Servos to the pan-tilt camera to simulate its motions of yaw and pitch, six “rotational” Servos to the joints and eight “rotational” Servos to the gripper for the manipulator to simulate its different poses, and several “rotational” Servos to the umbilical cable to simulate its motion when the ROV is under operation.

A Camera node is used to model a robot's on-board camera. The resultant image can be displayed on the 3D window. We applied a Camera node with color type to the pan-tilt camera to feedback information from the virtual world.

3. Operate the virtual underwater manipulator by using different modes

Operating the ROV to perform underwater operations smoothly is very challenging, so operational skills significantly impact the accuracy and efficiency of an operation. The developed virtual platform can provide an operator with a low-cost, convenient and safe training environment. It challenges an operator to proficiently coordinate the underwater manipulator, the submersible vehicle and the pan-tilt camera to accomplish operational tasks.

In order to offer the operator a multifunctional training platform, we operate the virtual underwater manipulator by using different modes. The modes to operate the underwater manipulator can be divided into remote operation and autonomous operation. The remote operational mode to the underwater manipulator mainly includes remotely operating the joints through joysticks (Sheikhbahaee et al., 2014), remotely operating the pose position and orientation of the end-effector through joysticks (Shim et al., 2010), and remotely operating the manipulator through a master arm (Jun et al., 2008). The joystick-based manipulator and the master arm-based manipulator are named switch manipulator and master-slave manipulator, respectively. The autonomous operational mode (Aggarwal and Albiez, 2013) to the underwater manipulator is usually combined with remote operation, as completely autonomous operation in underwater operations is difficult. The keyboard is used to remotely operate the virtual submersible vehicle and the virtual pan-tilt camera, as shown in Fig. 2. The keys in the magenta boxes are used to operate the submersible vehicle, including the following operations: surge, sway, heave, roll, pitch, yaw and hovering. The keys in the green box are used to operate the pan-tilt, including the following operations: yaw, pitch, stop motion and reset to initial pose.

3.1. Remotely operating the manipulator joints through the keyboard

Operating the underwater manipulator joints through joysticks is a common operational mode. It can make the end-effector have an ideal pose position and orientation when performing operational tasks. It is an effective operational mode when the manipulator meets the following characteristics: has fewer DOFs; has none or more than one inverse solutions at a given time. The operations of the virtual manipulator joints include azimuth, shoulder pitch, elbow pitch, forearm rotate, wrist yaw and wrist rotate. We use the keys in the red box on the keyboard to take the place of the joysticks to operate the virtual manipulator joints, as shown in Fig. 2. The keys in the cyan box are used for stopping the manipulator motion and opening/closing the gripper.

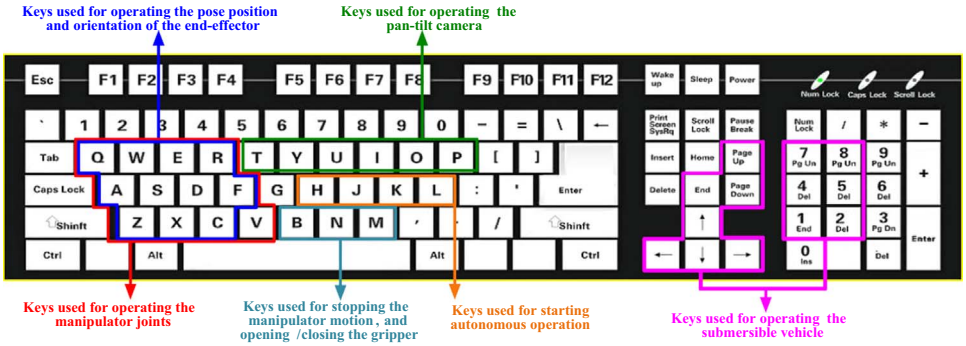

Fig. 2. Function assignment of keys on the keyboard. (For interpretation of the references to color in this figure, the reader is referred to the web version of this article).

If we want to know the pose position and orientation of the end-effector during operation, we can get it by solving the forward kinematics of the manipulator. We developed the manipulator kinematic model according to the D-H notation (Hartenberg and Denavit, 1955), which describes the spatial relationship between two adjacent links with a 4 × 4 homogeneous transformation matrix. We define the coordinate systems of connecting rods to the underwater manipulator with 7 functions (Fu, 1989), as shown in Fig. 3.

The parameters of each connecting rod to the manipulator are listed in Table 1, where i represents the number of the connecting rod, θ_i represents a rotation angle around the z^{i-1} axis to align the x^{i-1} and x^i axes, d_i represents a translation distance along the z^{i-1} axis to bring the x^{i-1} and x^i axes into coincidence, a_i represents a translation distance along x^i axis to bring the two origins into coincidence, and α_i represents a rotation angle around the x^i axis to make the two coordinate systems completely coincide.

The manipulator forward kinematics is to solve the pose position and orientation of the end-effector relative to the reference coordinate system through the corresponding homogeneous transformation matrix. The reference coordinate system is built on the base. The

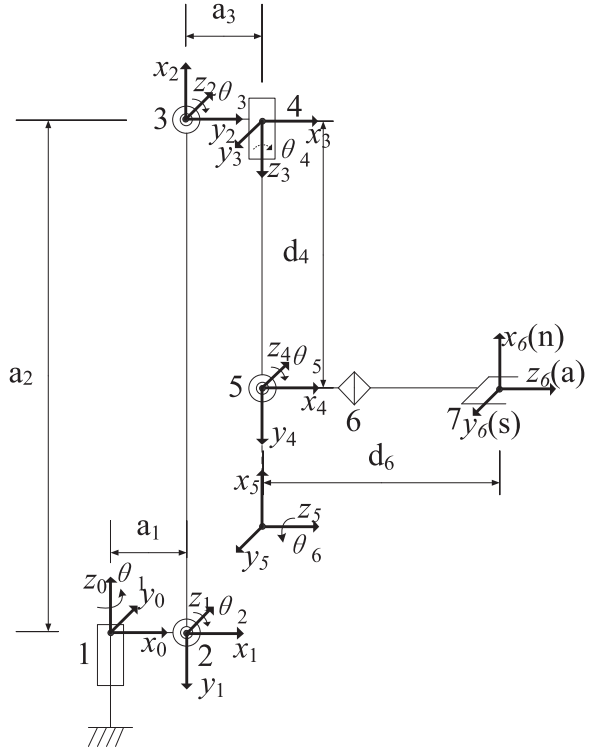

Fig. 3. Coordinate systems of the connecting rods to the underwater manipulator with 7 functions.

Table 1
Parameters of each connecting rod to the manipulator.

i	a_i/ (m)	α_i/ (deg.)	d_i/ (m)	θ_i/ (deg.)
1	0.096	−90	0	θ_1
2	0.932	0	0	θ_2
3	0.126	−90	0	θ_3
4	0	90	0.52	θ_4
5	0	−90	0	θ_5
6	0	0	0.461	θ_6

homogeneous transformation matrix ${}^{i-1}\mathrm{A}_i$ representing the relationship between ith and i^{-1}th coordinate system can be determined according to the defined D-H coordinate systems. It can be represented as follows:

$$
{}^{i-1}\mathrm{A}_i = \begin{bmatrix} \cos\theta_i & -\cos\alpha_i \sin\theta_i & \sin\alpha_i \sin\theta_i & a_i \cos\theta_i \\ \sin\theta_i & \cos\alpha_i \cos\theta_i & -\sin\alpha_i \cos\theta_i & a_i \sin\theta_i \\ 0 & \sin\alpha_i & \cos\alpha_i & d_i \\ 0 & 0 & 0 & 1 \end{bmatrix} = \begin{bmatrix} {}^{i-1}\mathrm{x}_i & {}^{i-1}\mathrm{y}_i & {}^{i-1}\mathrm{z}_i & {}^{i-1}\mathrm{p}_i \\ 0 & 0 & 0 & 1 \end{bmatrix} \tag{1}
$$

The 3 × 3 matrix $[{}^{i-1}\mathrm{x}_i\ {}^{i-1}\mathrm{y}_i\ {}^{i-1}\mathrm{z}_i]$ in Eq. (1) represents the orientation of the ith coordinate system relative to the i^{-1}th coordinate system. The vector ${}^{i-1}\mathrm{p}_i$ represents the origin of the ith coordinate system relative to i^{-1}th coordinate system. The transformation matrix of each connecting rod can be obtained by plugging the parameters in Table 1 into Eq. (1). We derive the homogeneous transformation matrix T of the end-effector coordinate system relative to the reference coordinate system according to the method in Fu (1989)

$$
\mathrm{T} = {}^{0}\mathrm{A}_1 {}^{1}\mathrm{A}_2 {}^{2}\mathrm{A}_3 {}^{3}\mathrm{A}_4 {}^{4}\mathrm{A}_5 {}^{5}\mathrm{A}_6 = \begin{bmatrix} n_x & s_x & a_x & p_x \\ n_y & s_y & a_y & p_y \\ n_z & s_z & a_z & p_z \\ 0 & 0 & 0 & 1 \end{bmatrix} \tag{2}
$$

For conveniently expressing Eq. (2), we replace sine(α_i) and cos(α_i) with −1, 0 or 1, and define the following notations:

$$n_x = C_1[C_{23}(C_4C_5C_6 - S_4S_6) - S_{23}S_5C_6] + S_1(S_4C_5C_6 + C_4S_6) \tag{3}$$

$$n_y = S_1[C_{23}(C_4C_5C_6 - S_4S_6) - S_{23}S_5C_6] - C_1(S_4C_5C_6 + C_4S_6) \tag{4}$$

$$n_z = -S_{23}(C_4C_5C_6 - S_4S_6) - C_{23}S_5C_6 \tag{5}$$

$$s_x = C_1[-C_{23}(C_4C_5S_6 + S_4C_6) + S_{23}S_5S_6] + S_1(-S_4C_5S_6 + C_4C_6) \tag{6}$$

$$s_y = S_1[-C_{23}(C_4C_5S_6 + S_4C_6) + S_{23}S_5S_6] - C_1(-S_4C_5S_6 + C_4C_6) \tag{7}$$

$$s_z = S_{23}(C_4C_5S_6 + S_4C_6) + C_{23}S_5S_6 \tag{8}$$

$$a_x = -C_1(C_{23}C_4S_5 + S_{23}C_5) - S_1S_4S_5 \tag{9}$$

$$a_y = -S_1(C_{23}C_4S_5 + S_{23}C_5) + C_1S_4S_5 \tag{10}$$

$$a_z = S_{23}C_4S_5 - C_{23}C_5 \tag{11}$$

$$p_x = -C_1[d_6(C_{23}C_4S_5 + S_{23}C_5) + S_{23}d_4 - a_2C_2 - a_3C_{23} - a_1] - S_1S_4S_5d_6 \tag{12}$$

$$p_y = -S_1[d_6(C_{23}C_4S_5 + S_{23}C_5) + S_{23}d_4 - a_2C_2 - a_3C_{23} - a_1] + C_1S_4S_5d_6 \tag{13}$$

$$p_z = d_6(S_{23}C_4S_5 - C_{23}C_5) - C_{23}d_4 - a_2S_2 - a_3S_{23} \tag{14}$$

where $C_i \equiv \cos\theta_i$, $S_i \equiv \sin\theta_i$, $C_{ij} \equiv \cos(\theta_i+\theta_j)$, and $S_{ij} \equiv \sin(\theta_i+\theta_j)$.

After we solved the pose position and orientation of the end-effector in real time, the end-effector trajectory during operation can be obtained.

3.2. Remotely operating the pose position and orientation of the end-effector through the keyboard

Sometimes, operating the pose position and orientation of the end-effector is a more direct and faster mode when performing operational tasks. Especially for a case such that the manipulator has more DOFs and at least one inverse solution at all times. The operations of directly operating the manipulator end-effector include gripper forwards, gripper backwards, gripper strafe left, gripper strafe right, gripper rise, gripper fall, gripper rotate left, gripper rotate right, gripper direction along x axis, gripper direction along y axis, gripper direction along z axis. We use the keys in the blue box on the keyboard to take the place of the joysticks to operate the virtual manipulator end-effector, as shown in Fig. 2.

Giving the pose position and orientation of the end-effector, solving θ_i yields the analytical solution to the manipulator inverse kinematics. The method proposed in Huo et al. (2013), combined with the characteristics of the Euler method and the geometric method, can be used to solve the inverse kinematics of the underwater manipulator. The results are as follows:

$$\theta_1 = \arctan(p_y/p_x) \tag{15}$$

$$\theta_2 = -\arctan\left(p_z/(\sqrt{p_x^2+p_y^2} - a_1)\right) - \arccos\left(\frac{a_2^2 + (\sqrt{p_x^2+p_y^2} - a_1)^2 + p_z^2 - (a_3^2+d_4^2)}{2a_2\sqrt{(\sqrt{p_x^2+p_y^2} - a_1)^2 + p_z^2}}\right) \tag{16}$$

$$\theta_3 = \pi - \arctan(d_4/a_3) - \arccos\left(\frac{a_2^2 + (a_3^2+d_4^2) - \left((\sqrt{p_x^2+p_y^2} - a_1)^2 + p_z^2\right)}{2a_2\sqrt{a_3^2+d_4^2}}\right) \tag{17}$$

$$\theta_4 = tg^{-1}2(a_{4y}, a_{4x}) \tag{18}$$

$$\theta_5 = -tg^{-1}2(C_4a_{4x} + S_4a_{4y}, a_{4z}) \tag{19}$$

$$\theta_6 = tg^{-1}2(-S_4n_{4x} + C_4n_{4y}, -S_4s_{4x} + C_4s_{4y}) \tag{20}$$

where $(p_x, p_y, p_z)^T$ represents the origin of the wrist, it is a position vector relative to the referenced coordinate system; $[n_{4x}\ s_{4x}\ a_{4x};\ n_{4y}\ s_{4y}\ a_{4y};\ n_{4z}\ s_{4z}\ a_{4z}]$ represents the orientation of the end-effector coordinate system relative to the fourth coordinate system at zero position. The results of θ_4, θ_5 and θ_6 are confined between $-\pi$ and π through the function of $tg^{-1}2(y, x)$, which is expressed as follows:

Fig. 4. The master arm.

$$tg^{-1}2(y, x) = \begin{cases} 0° \le \theta \le 90° & x+, y+ \\ 90° \le \theta \le 180° & x-, y+ \\ -180° \le \theta \le -90° & x-, y- \\ -90° \le \theta \le 0° & x+, y- \end{cases} \tag{21}$$

The end-effector trajectory can be obtained directly during an operation when the manipulator is operated by the end-effector. We can determine the rotational angles of each joint at all times by solving the manipulator inverse kinematics.

3.3. Remotely operating the manipulator through the master arm

The master arm-based operational mode is usually used to remotely operate the manipulator for underwater operations due to its intuition and reliability. It is using a miniature replica master arm to operate the manipulator as a slave arm. This paper established a master-slave manipulator system, in which the operator used a real master arm to remotely operate the virtual manipulator. The master arm is shown in Fig. 4, which is a functional replica of the manipulator. The master arm allows for easy control of the functions with a shoulder, an elbow, a forearm, and a wrist. The auxiliary gripper switch at the left of the screen controls a gripper state, e.g., moving the switch forward closes the gripper and moving the switch rearward opens the gripper. The button at the tip of the master arm is used to freeze/unfreeze the master arm.

The relative position incremental method was used to control the manipulator (Kuo and Tal, 1979). The rules for controlling the slave arm joints by the master arm joints are given below

$$S_{icmd} - S_{iref} = k_i(M_{iact} - M_{iref}) \qquad (i = 1, 2, \ldots, 6) \tag{22}$$

$$k_i = (S_{i\,\max} - S_{i\,\min})/(M_{i\,\max} - M_{i\,\min}) \tag{23}$$

where S_{icmd} is a setting angle that the ith slave manipulator joint needs to reach, S_{iref} is the current angle of the ith slave manipulator joint that is used as a reference, M_{iact} is the actual angle of the ith master arm joint, M_{iref} is the reference angle at which the ith master arm joint was situated in last step, k_i represents the proportional coefficient of the incremental controller between the ith slave manipulator joint and the ith master arm joint, M_{imax}/M_{imin} is the ratio of the maximum angle over the minimum angle of the ith master arm joint, and S_{imax}/S_{imin} is the ratio of the maximum angle over the minimum angle of the ith slave manipulator joint. The rules for controlling the gripper is similar to the joints.

Similarly, we can get the end-effector trajectory during operation by solving the forward kinematics of the manipulator.

3.4. Operating the manipulator by combining remote operation with autonomous operation through the keyboard

Remote operation is widely used in underwater operational tasks as

the sea environment is complex. However, the operator usually has a larger operating pressure when using this mode to do tasks. In addition, the remote operational mode cannot meet the requirements for tasks where higher operational quality and precision are required. The recent development of autonomous underwater vehicles (AUVs) indicate a growing interest in expanding the vehicles capabilities with intervention skills. The so-called intervention AUV is trying to incorporate one or more manipulators to the submersible with the objective of performing complex autonomous tasks. The main advantage of such an intervention AUV would be its lower operational cost. Some AUVs equipped with manipulator arms have demonstrated the progress (Sverdrup-Thygeson et al., 2016; Palomeras et al., 2016; Ribas et al., 2012). The autonomous operation certainly reduces the pressure of operators, but until now there are very few examples of fully autonomous manipulator operation successfully to do tasks in a complex environment. The question is that any task that nowadays need manned submersible vehicles or ROVs is complex and the sensor availability is very limited.

Given the continued growth in the ROV industry and the work load currently experienced by ROV crews, there is an imminent need for semi-autonomous ROVs (Proctor et al., 2015; Proctor, 2014; Fossum et al., 2016). In a semi-autonomous configuration, the operator directly provides high-level position commands and the low level controller autonomously compensate for the environmental disturbances and unknown dynamics (such as current and tether dynamics), which allows the operator to focus on other aspects of the task (such as manipulator control). For example, important application is to achieve the autonomously stationary keeping of ROV statuses so that the operator is able to concentrate on task manipulation. Generally speaking, semi-autonomous ROV operations can alleviate and simplify the mission complexity, making the operation less dependent on operator skills, whilst providing increased precision, and reduced operating time.

In this paper, we referred to the idea of semi-autonomous ROV operations and combined remote operation with autonomous operation to operate the underwater manipulator. It can not only ensure the operational ability for the manipulator, but also can reduce the operating pressure and improve the operational efficiency and precision for the operator. We can use the autonomous operational mode to operate the manipulator for the process when the end-effector trajectory or the manipulator pose can be determined. For example, the process of making the end-effector approach the target (the end-effector trajectory can be determined if the target position can be roughly positioned through sensors), the process to operate the target (the end-effector trajectory can be determined if the operating process to the target is fixed), the process to place the object on the basket (the manipulator pose can be determined), and the process to reset the manipulator to its initial pose (the manipulator pose is determined) can use the mode of autonomous operation. When tasks are conducted by the autonomous operational mode, the operator just need to directly provide high-level behavior commands as in semi-autonomous ROV operations, and then the low level controller will autonomously perform operations regarding the underwater manipulator. The keys in the orange boxes are used to start autonomous operation, including starting the four autonomous operational processes mentioned above. While for the process when the end-effector trajectory or the manipulator pose cannot be determined, the mode of remotely operating the pose position and orientation of the end-effector through the keyboard can be used to operate the manipulator. When tasks are conducted by the remote operational mode, the operator need to focus on manipulator control, such as operating or adjusting the pose of the manipulator step by step in real-time.

4. Uncertain external disturbance

Because of the ocean currents in the subsea environment, disturbances to the ROV should be considered. The disturbances make the end-effector of the manipulator shake constantly, which will increase the difficulty of performing operational tasks. In order to make the training processes more effective, a random disturbance in 3D space should be added to the virtual ROV. The added disturbance is only aimed at increasing the difficulty of the operation and providing a more effective training platform, which has lower requirements in accuracy and authenticity. To generalize, the fluid flow impact is also a very complicated and time-consuming computational process. So a random disturbance in horizontal and vertical directions, modeled by two 2D sine waves, were added by us to the ROV to simulate the disturbance effect in 3D space. We can provide different disturbance effects in 3D space by adjusting disturbance ranges of the two 2D sine waves. A response curve, following the sine function with a period of 4 s, is used to describe the pitch moment of an underwater vehicle in Malik et al. (2013). The random disturbance refers to the curve, which is represented as follows:

$$\begin{bmatrix} \theta_{\text{pitch}} \\ d_{\text{sway}} \end{bmatrix} = \begin{bmatrix} r_1 \sin(\pi t/2) \\ r_2 \sin(\pi t/2) \end{bmatrix} \tag{24}$$

where θ_{pitch} and d_{sway} represent the disturbance from pitch and sway, r_1 represents the pitch disturbance range with units of degrees, r_2 represents the sway disturbance range with units of millimeters, t represents working time with units of seconds. For training purposes, the sine wave-based disturbances challenges an operator to achieve a desired operation performance under uncertainties.

5. Platform validation and experiment

In order to validate the feasibility and effectiveness of the virtual training platform, three operators were invited to perform tasks on it. They operated the virtual underwater manipulator using different modes to perform two typical underwater operational tasks: (1) Grasping a machine part in a basket; (2) making a circle at a specified position on the seabed. These two tasks represent the basic task types in underwater operations. The disturbance added to the ROV is based on Eq. (24) with $r_1 = 1°$ and $r_2 = 35$ mm. Other settings can be made to the Webots world to simulate the seabed environment, such as setting the light direction, the background color, the seabed surface pattern, etc.

A controller is a computer program that controls a virtual robot specified in a world file. We developed a controller in the C language named “mybot” to control the virtual ROV. When a simulation starts, Webots will launch the “mybot” controller, and it will associate the controller with the virtual ROV. After the “mybot” controller receives instructions from the operating equipment, it calls the corresponding function to perform the desired operations.

5.1. Grasping a machine part in a basket

The first task presented herein is operating the ROV to grasp a machine part in a basket, which is a common operational task. The operator usually has difficultly in quickly grasping the machine part with an ideal manipulator pose when doing this task, especially in the case where the ROV is disturbed in the subsea environment. The requirement in operational precision is lower and the end-effector trajectory can not be determined during the operation for this task, so the remote operational mode is usually used to do it. The process is described as follows: (1) Operate the pan-tilt camera to search for the machine part in the basket; (2) Pilot the ROV to approach the basket and ensure that the target is within the workspace of the manipulator; (3) Operate the manipulator to grasp the machine part from its initial pose, and pay attention to the grasp direction and the grasp timing; (4) Reset the manipulator to its initial pose after completing the task. We use different modes of remote operation to operate the manipulator in this task. We should make the operators know the function assignment

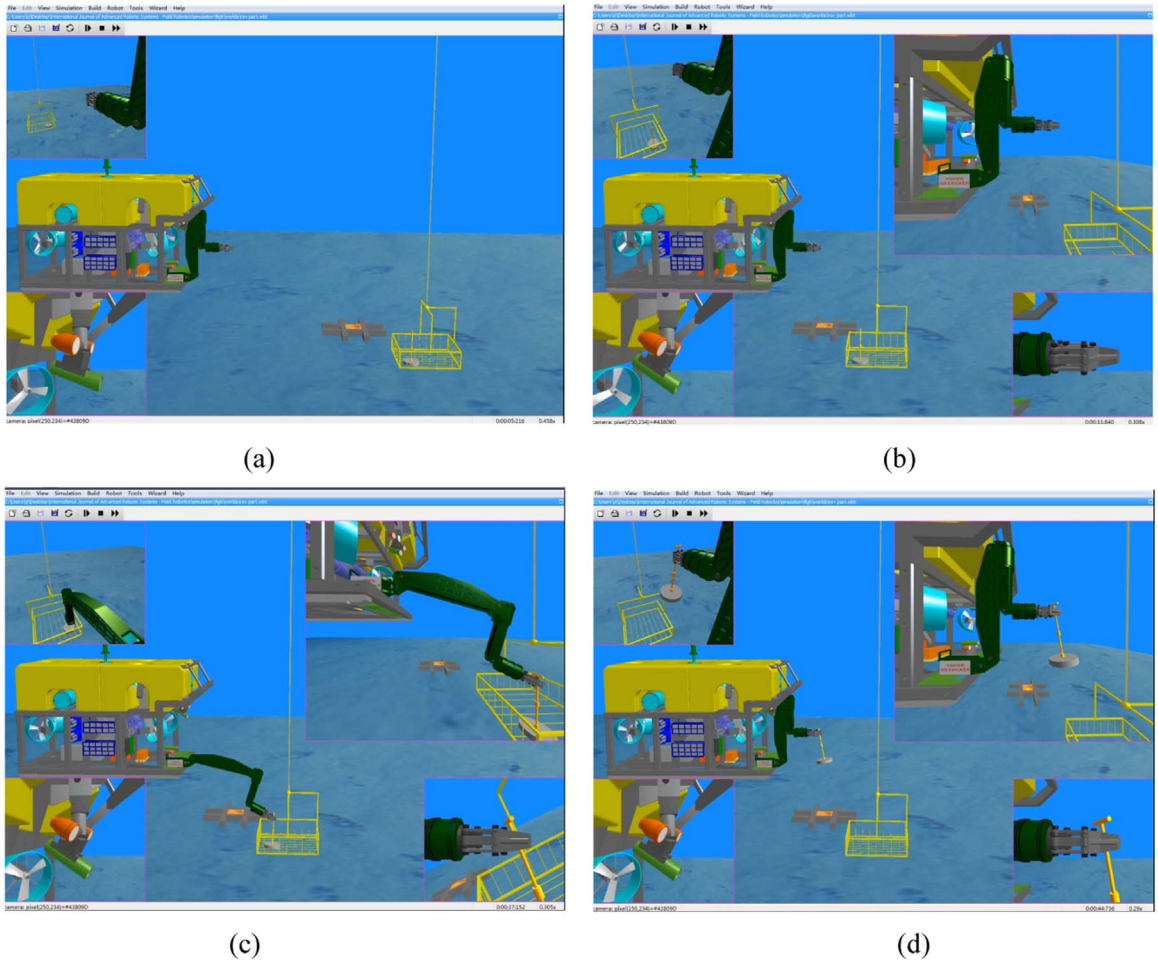

Fig. 5. The process of grasping a machine part in a basket. The manipulator is remotely operated by joints through the keyboard.

of the keys on the keyboard and the usage of the master arm before doing the task.

Fig. 5(a)–(d) show the process of doing this task when the manipulator is remotely operated by joints through the keyboard. The upper-left window, upper-right window, lower-left window, and lower-right window of Fig. 5(b) show the surroundings' information taken by the pan-tilt camera, motion of the underwater manipulator, motions of the pan-tilt camera and headlamps, and motion of the gripper, respectively.

Fig. 6 shows the end-effector trajectories when operating the manipulator by using different operational modes during the task. They were all generated by the operator who used the intermediate operating time among the three operators in different operational modes. Fig. 6(a) shows the end-effector trajectory of operating the manipulator joints through the keyboard, Fig. 6(b) shows the end-effector trajectory of operating the pose position and orientation of the end-effector through the keyboard, and Fig. 6(c) shows the end-effector trajectory of operating the manipulator through the master arm. The manipulator was reset to its initial pose by using the mode of autonomous operation when using the keyboard to operate the manipulator. While the manipulator was reset to its initial pose by directly operating the master arm when using the master arm to operate the manipulator. The average operating time (including the time of operating the submersible vehicle and the pan-tilt camera) for successfully completing the task by using the three different operational modes for the three operators were t_1 = 99 s, t_2 = 66 s, and t_3 = 64 s, respectively. Please note that the disturbance increased the operating time.

Fig. 7(a) shows the distance (the end-effector to the grasped position on the machine part) changes along with time for the operating results of Fig. 6. The black curve is the change in distance, represented by d_1, for the operating result of Fig. 6(a). The total path length, the operating time, and the time to reach the grasped position for the manipulator are 5.67 m, 71 s, and 40 s, respectively. The magenta curve is the change in distance, represented by d_2, for the operating result of Fig. 6(b). The total path length, the operating time, and the time to reach the grasped position for the manipulator are 4.24 m, 45 s, and 24 s, respectively. The blue curve is the change in distance, represented by d_3, for the operating result of Fig. 6(c). The total path length, the operating time, and the time to reach the grasped position for the manipulator are 4.32 m, 46 s, and 18 s, respectively. Fig. 7(b) shows the change in velocity magnitude of the end-effector along with time for the operating results of Fig. 6. The black curve is the change in velocity magnitude, represented by v_1, for the operating result of Fig. 6(a). The average velocity magnitude is 0.080 m/s. The magenta curve is the change in velocity magnitude, represented by v_2, for the operating result of Fig. 6(b). The average velocity magnitude is 0.094 m/s. The blue curve is the change of velocity magnitude, represented by v_3, for the operating result of Fig. 6(c). The average velocity magnitude is 0.094 m/s.

From Fig. 7 we can see that operating the manipulator joints through the keyboard has a lower operational efficiency as the manipulator has more DOFs. The mode of operating the manipulator through the master arm is the first to grasp the machine part in the three different operational modes, but it spends more time on resetting the manipulator to its initial pose, so the mode of autonomous operation is more efficient than the mode of operating

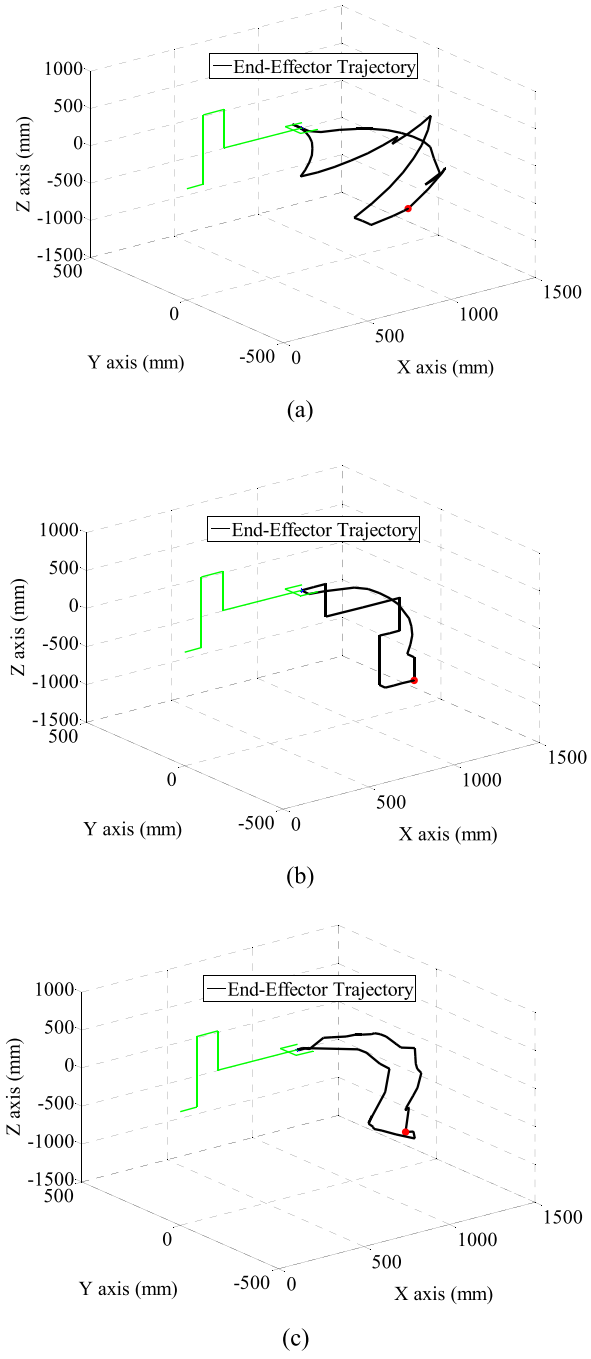

Fig. 6. (a) The end-effector trajectory of operating the manipulator joints through the keyboard during task. (b) The end-effector trajectory of operating the pose position and orientation of the end-effector through the keyboard during task. (c) The end-effector trajectory of operating the manipulator through the master arm during task. The green lines represent the manipulator which is shown at its initial pose. The red point represents the grasped position on the machine part. (For interpretation of the references to color in this figure legend, the reader is referred to the web version of this article).

through the master arm when resetting the manipulator to its initial pose. The distances of the end-effector to the grasped position usually stay at zero for a short time, while the manipulator is grasping the machine part. The sharp turning points in the robot trajectories where the velocity magnitudes are nearly zero usually happens. Every operating result provides a reference as to verify whether each operator improves his/her performance while conducting the next operation.

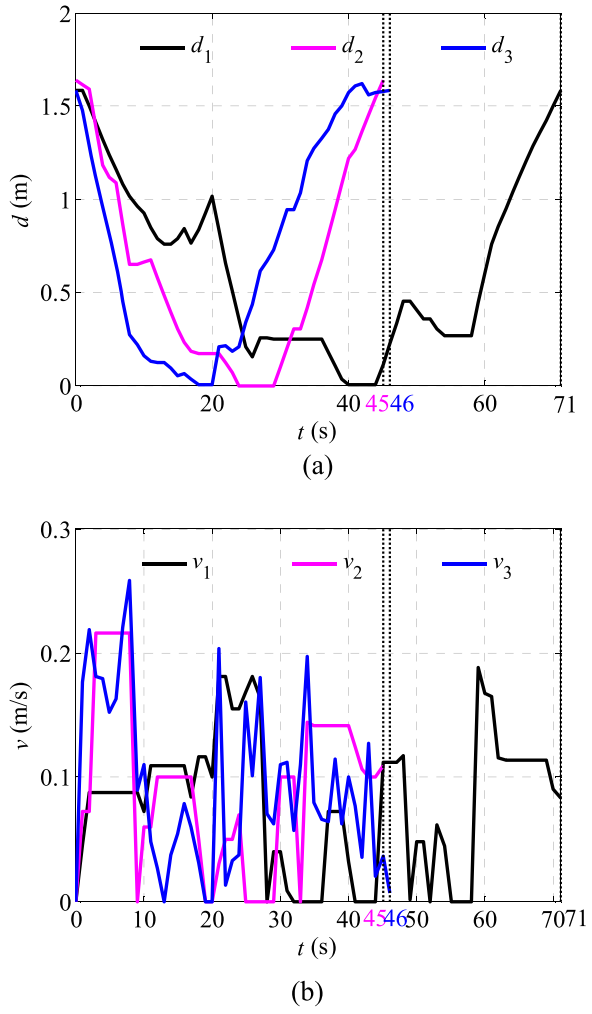

Fig. 7. (a) The distance (the end-effector to the grasped position on the machine part) changes along with time for the operating results of Fig. 6. (b) The velocity magnitude changes of the end-effector along with time for the operating results of Fig. 6. The black curves are the operating result of Fig. 6(a), the magenta curves are the operating result of Fig. 6(b), and the blue curves are the operating result of Fig. 6(c). (For interpretation of the references to color in this figure legend, the reader is referred to the web version of this article).

5.2. Making a circle at a specified position on the seabed

The second task presented herein is making a circle at a specified position on the seabed. This task is a representative type of underwater operation with higher requirements in operation quality and precision. The operator will not have an ideal operating result if only remote operational mode is used. In the virtual world, an object on the seabed is added for specifying the position needed to be marked, a pen gripped by the gripper is added for marking the circle, a basket is added for holding the pen after completing the mark, and two cameras are added for roughly positioning the object. The operational process is described as follows: (1) Operate the pan-tilt camera to search for the object which specified the position needed to be marked; (2) Pilot the ROV to approach the object and ensure that the object is within the workspace of the manipulator; (3) Operate the manipulator to make its end-effector approach the object from its initial pose; (4) Operate the manipulator to make its end-effector have an ideal pose position and orientation to mark the circle; (5) Operate the manipulator to mark the circle around the object by using the pen; (6) Operate the manipulator to place the pen in the basket after completing the mark; (7) Reset the manipulator to its initial pose after completing the task. Some of the end-effector trajectories and manipulator poses can be determined during the process of doing this task, so the mode of

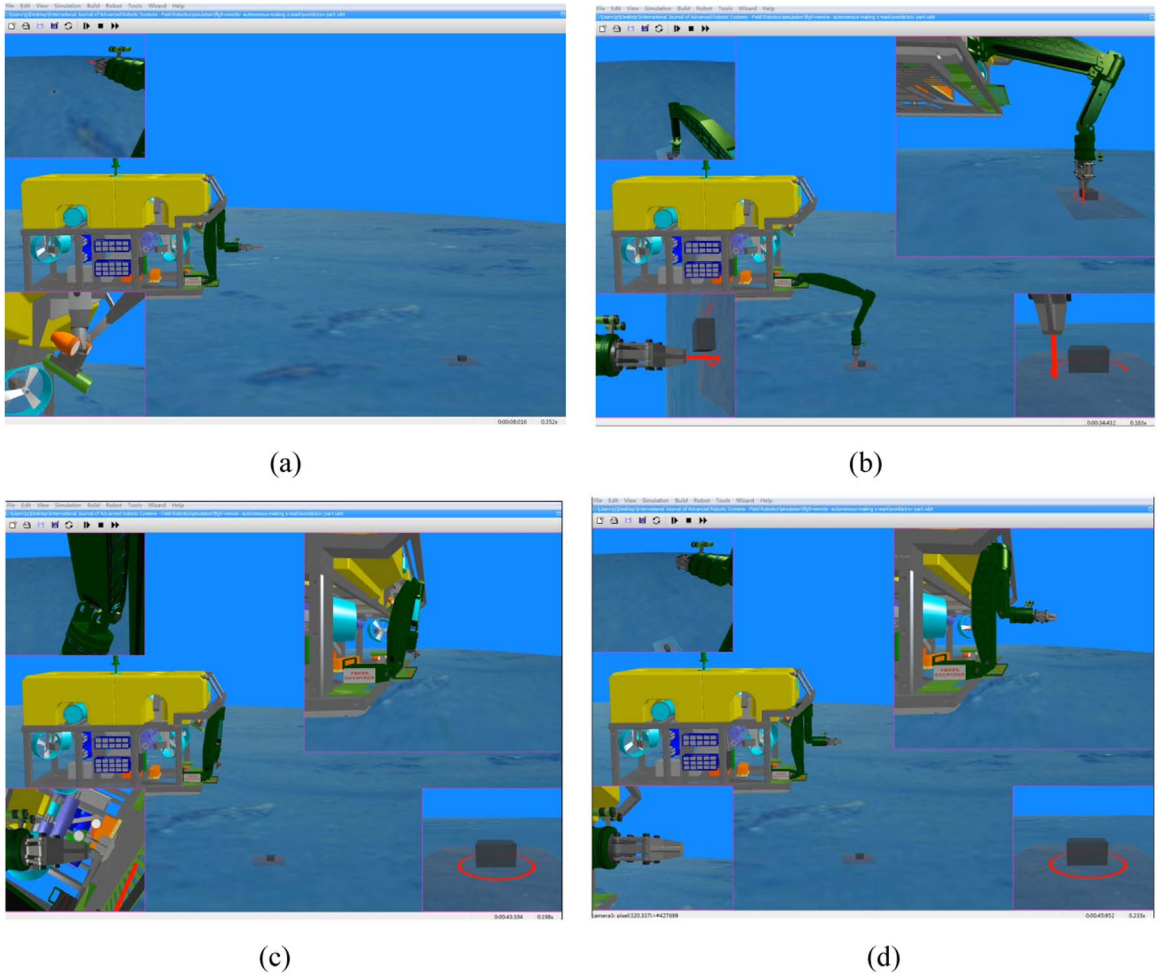

Fig. 8. The process of making a circle at a specified position on the seabed performed by one of the three operators.

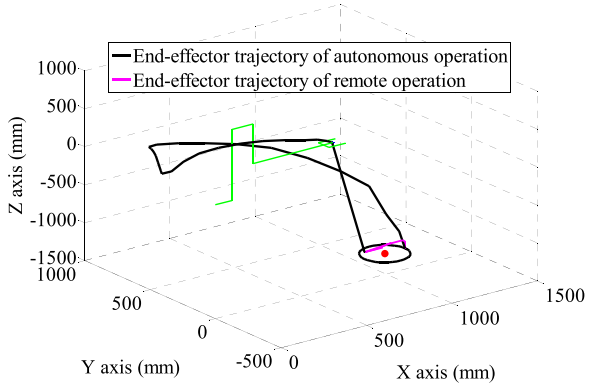

Fig. 9. The end-effector trajectory during the task. The black curve and magenta curve are the end-effector trajectories of autonomous operation and remote operation, respectively. The red point is the object position. (For interpretation of the references to color in this figure legend, the reader is referred to the web version of this article).

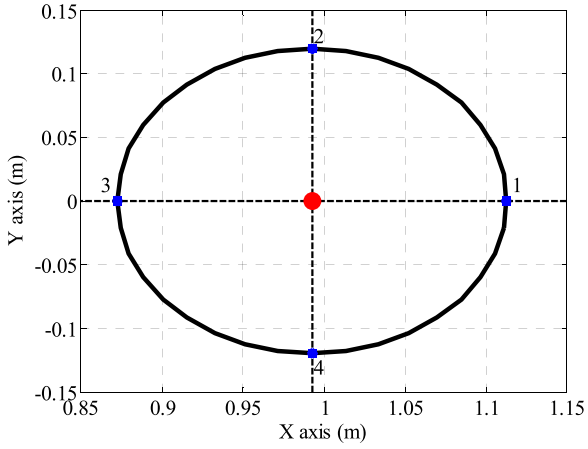

Fig. 10. Marking results of making a circle at a specified position on the seabed. It's a circle with a radius of 0.12 m.

combining remote operations with autonomous operations to operate the manipulator can be used in this task, which can reduce the operating pressure and improve the operational efficiency and precision. Because the object position can be roughly positioned by the two cameras, we can make the manipulator end-effector approach the object along a straight line in step (3). So the end-effector trajectories of the manipulator can be determined in step (3) and step (5), the mode of autonomous operation to the manipulator can be used in these two steps. As the end-effector trajectory or the pose of the manipulator cannot be determined in step (4), we can use the mode of remotely operating the pose position and orientation of the end-effector to operate the manipulator in this step. The poses of the manipulator can be determined in step (6) (60°, −75°, 85°, −45°, −35°, 0°) and step (7) (0°, −90°, 90°, 0°, −90°, 0°), so the mode of autonomous operation to the manipulator can be used in these two steps. We should let the operator know the function assignment of the keys on the keyboard before doing the task.

Table 2
end-effector positions at the four blue points and their corresponding joint angles.

i	End-effector position (m)			Joint angles (deg.)					
	x	y	z	θ_1	θ_2	θ_3	θ_4	θ_5	θ_6
1	1.11	0.00	−1.23	0.00	15.14	−14.13	0.00	−1.01	0.00
2	0.99	0.12	−1.23	6.89	14.32	−0.77	0.00	−13.55	6.89
3	0.87	0.00	−1.23	0.00	15.23	11.66	0.00	−26.89	0.00
4	0.99	−0.12	−1.23	−6.89	14.32	−0.77	0.00	−13.55	−6.89

Fig. 8(a)–(d) show the process of doing this task performed by one of the three operators. The upper-left window, upper-right window, lower-left window, and lower-right window of Fig. 8(b) show the surrounding information taken by the pan-tilt camera, motion of the underwater manipulator, motion of the gripper, and the position needed to be marked, respectively.

Fig. 9 shows the end-effector trajectory during the task. For obtaining a regular circle, there is no disturbance added to the ROV when the manipulator is drawing the circle. The black curve and magenta curve are the end-effector trajectories of autonomous operation and remote operation, respectively. His operating time to the manipulator is 134 s, including 102 s of autonomous operation and 32 s of remote operation. From Fig. 9 we can see that the marking task is well done through the operational mode of combining remote operation with autonomous operation. The task was completed precisely and efficiently. This task can train an operator to do tasks of operating the manipulator by the mode of combining remote operation with autonomous operation.

Fig. 10 shows the marking results for this task, which is a circle with a radius of 0.12 m. We need to solve the manipulator inverse kinematics in real-time to obtain a set of corresponding poses while drawing the circle. The drawing result validates the effectiveness of the algorithm proposed in Huo et al. (2013). The end-effectors are positioned at the four blue points and their corresponding joint angles are listed in Table 2, where i (i = 1, 2, 3, 4) represents the point number. So the virtual platform is also an economic and safe tool for testing and validating motion control methods of the underwater manipulator.

The two experimental results show that the platform provides operators with an effective training environment and is also a valuable tool for testing and validating motion control methods for manipulators. Before the three operators used the virtual platform for training the first time, we needed to explain to them the detailed training process and the matters needing attention during the operation. Their operating time of completing tasks is decreased through repeated training, while their operating quality steadily increased. A new operator usually has a psychological burden so that he/she does not dare to operate a real manipulator the first time, because he/she may worry about damaging the equipment. However, the training platform gives them the confidence to operate the real manipulator.

6. Conclusion

Until now, there are no examples of using real ROV systems to train operators and to evaluate their operational performance in the real world, because it is impossible to duplicate their operational processes under the uniform conditions. In addition, it does not suit to train the operators by adjusting external disturbances and select operational modes of the underwater manipulator by using real ROV systems. The developed virtual platform in this paper provides an operator an effective and economic training environment to investigate a variety of manipulator operations.

The existing virtual platforms for ROVs, used for training operators, are different from the platforms developed in this paper in their mechanical structures for submersible vehicles and underwater manipulators. Specifically, they do not provide the training process and resulting analysis of the procedure. In this paper, we presented the training process of the developed virtual platform and the operation results of two typical tasks by taking external disturbances into account while conducting tasks. The experimental results demonstrate the feasibility and effectiveness of our virtual platform. In addition, the virtual platform can not only be used to test and validate motion control methods for operating the submersible vehicle and manipulator (Jun et al., 2008; Li and Wan, 2011), but also it can be used as an auxiliary control system to display the motion state and trajectory of the real submersible vehicle and underwater manipulator where the developers do not have a direct view of the system (Ge and Guo, 2012).

At the current stage, we simplify the control process of the manipulator with the many DOFs mounted on the ROV with the complex structure to find out the main issues how to effectively train an operator using the developed virtual platform. In order to short computational times, we made the following assumptions: 1) The model in Webots doesn't include the hydrodynamic model of the ROV and the manipulator; 2) The whole system assumed to be neutrally buoyant; 3) The motion of the manipulator is assumed to have no influence on the motion of the ROV; 4) The control of the position of the ROV is considered as low priority task; 5) The autonomous control tasks are purely kinematic. How does these simplifications could impact on training process will be fully considered after performing real underwater experiments. Then, the virtual platform will be improved accordingly.

References

Aggarwal A., Albiez J., 2013. Autonomous trajectory planning and following for industrial underwater manipulators. In: Proceedings of the Oceans. 2013, IEEE, San Diego, pp. 1–7.

Chi, Y., 2013. Research on operation scene simulation technology of ROV. Harbin Eng. Univ..

Fossum T.O., Ludvigsen M., Nornes S.M.. et al., 2016. Autonomous robotic intervention using ROV: an experimental approach. In: Proceedings of the Oceans. IEEE, Monterey, CA, USA.

Fu, J.S., 1989. Robotics: Control, Sensing, Vision, and Intelligence. China Science and Technology Press, Beijing, 26–31.

Ge, X., Guo, W., 2012. Design of assisted control system of ROV based on virtual reality. Mach. Des. Manuf. 11, 91–93.

GRI Simulations Inc, 2015. In Manipulator Trainer, Mt Pearl. [Online]. Available: ⟨http://www.grisim.com/products.html#ManipTrainer⟩.

Hamzah M., Salzahrin M., Zakaria M.. et al., 2008. 3D Virtual Simulation Software for Underwater Application.

Hartenberg, R.S., Denavit, J., 1955. A kinematic notation for lower-pair mechanisms based on matrices. J. Appl. Mech. 22, 215–221.

Huo, L.Q., Zhang, Q.F., Zhang, Z.Y., 2013. A method of inverse kinematics of a 7-function underwater hydraulic manipulator. In: Proceedings of the Oceans'13 MTS/IEEE. New York, USA, pp. 1–4.

Jun, B.H., Lee, P.M., Kim, S., 2008. Manipulability analysis of underwater robotic arms on ROV and application to task-oriented joint configuration. J. Mech. Sci. Technol. 22, 887–894.

Koivumäki, Janne, Mattila, Jouni, 2016. Stability-guaranteed impedance control of hydraulic robotic manipulators. IEEE/ASME Trans. Mechatron..

Kuo, B.C., Tal, J. (Eds.), 1979. Incremental Motion Control. SRL Publishing Co., Champaign, III..

Li, J.Q., Wan, L., 2011. The heel and trim adjustment of manned underwater vehicle based on variable universe fuzzy S surface control. In: Proceedings of the 2011 International Conference on Electronics, Communications and Control (ICECC).

IEEE, Ningbo, China, pp. 1122–1125.
Lorance, P., Trenkel, V.M., 2006. Variability in natural behavior, and observed reactions to an ROV, by mid-slope fish species. J. Exp. Mar. Biol. Ecol. 332, 106–119.
Malik, S.A., Pan, G., Liu, Y.A., 2013. Numerical simulations for the prediction of wave forces on underwater vehicle using 3D panel method code. Res. J. Appl. Sci. Eng. Technol. 5, 5012–5021.
Michel, O., 2004. Cyberbotics Ltd – WebotsTM: professional mobile robot simulation. Int. J. Adv. Robot. Syst. 1 (1), 40–43.
Narayanaswamy, V., Raju, R., Durairaj, M., et al., 2013. Reliability-centered development of deep water ROV ROSUB 6000. Mar. Technol. Soc. J. 47, 55–71.
Palomeras, N., Peñalver, A., Massot-Campos, M., et al., 2016. I-AUV docking and panel intervention at sea. Sensors 16 (10), 1673.
Park, S.J., Yeu, T.K., Yoon, S.M., Hong, S., Sung, K.Y., 2011. A study of sweeping coverage path planning method for deep-sea manganese nodule mining robot. In: Proceedings of the OCEANS 2011. IEEE, Waikoloa, Hawaii, USA, pp. 1–5.
Proctor, A.A., Buchanan, A., Buckham, B., Bradley, C., 2015. ROVs with semi-autonomous capabilities for use on renewable energy platforms. In: Proceedings of the Twenty-fifth (2015) International Ocean and Polar Engineering Conference. Hawaii, USA, pp. 629–636.
Proctor, Alison A., 2014. Semi-autonomous guidance and control of a Saab Seaeye Falcon ROV. Auton. Veh..
Ribas, D., Palomeras, N., Ridao, P., et al., 2012. Girona 500 AUV: from survey to intervention. IEEE/ASME Trans. Mechatron. 17, 46–53.
SeaVeyors Environmental and Marine Services Limited, 2015. ROV Operations. [Online]. Available: ⟨http://www.seaveyors.ca/services/rov-operations⟩.
Sheikhbahaee, Hamed, Mostashfi, Amir, Madhkhan, Mojtaba, Esmaelean, Mostafa, 2014. Development of a four-DOF laboratory underwater manipulator for using in towing tank. Indian J. Sci. Res 1, 895–899.
Shim, H., Jun, B.H., Lee, P.M., et al., 2010. Workspace control system of underwater tele-operated manipulators on an ROV. Ocean Eng. 37, 1036–1047.
Sverdrup-Thygeson, J., Kelasidi, E., Pettersen, K.Y., et al., 2016. The underwater swimming manipulator – a bio-inspired AUV. In: Proceedings of the IEEE OES Autonomous Underwater Vehicles. IEEE, Tokyo, Japan, pp. 387–395.
Wang, Y., et al., 2016. Development of an underwater manipulator and its free-floating autonomous operation. IEEE/ASME Trans. Mechatron. 21, 815–824.
Webots. ⟨http://www.cyberbotics.com/webots.php⟩. Commercial Mobile Robot Simulation Software.
Yan, Y., Ma, P.S., Wang, D.Y., Gao, X.G., 2005. Development of deep sea ROV and its working system. ROBOT. Vol. 27, pp. 82–89, Jan. 2005.
Zhang, Q.F., Zhang, Y.X., Huo, L.Q.. et al., 2014. Design and pressure experiments of a deep-sea hydraulic manipulator system. Intelligent Robotics and Applications. Springer International, Guangzhou, China, Dec. 2014,pp. 117–128.